Effect of Ethanol and Iso-octane Blends on Isolated Low Temperature Heat Release in a Spark Ignition Engine

Samuel P. White[a], Abdulah U. Bajwa[a], Felix C.P. Leach[a,*]

[a]*Department of Engineering Science, University of Oxford, Oxford, OX1 3PJ, UK*

Abstract

Low temperature heat release (LTHR) is of interest for its potential to help control autoignition in advanced compression ignition (ACI) engines and mitigate knock in spark ignition (SI) engines. Previous studies have identified and investigated LTHR in both ACI and SI engines before the main high temperature heat release (HTHR) event and, more recently, LTHR in isolation has been demonstrated in SI engines by appropriately curating the in-cylinder thermal state during compression and disabling the spark discharge. Ethanol is an increasingly common component of market fuel blends, owing to its renewable sources. In this work, the effect of adding ethanol to iso-octane (2,2,4-trimethylpentane) blends on their LTHR behaviour is demonstrated. Tests were run on a motored single-cylinder engine with inlet air temperatures and pressures were adjusted to realise LTHR from blends of iso-octane and ethanol without entering the HTHR regime. The blends were tested with inlet temperatures of 40 °C to 140 °C at equivalence ratios of 0.5, 0.67 and 1.0 with boosted (1.5 barA) conditions. The measured LTHR decreased with increasing ethanol content for all conditions tested; iso-octane-ethanol blends with above 20% ethanol content (by volume) showed minimal LTHR under engine conditions. These net effects resulted from the combination of thermal effects (charge cooling) and chemical effects (reactivity changes at low temperatures). The effect of temperature, pressure, fuel composition, and equivalence ratio on ignition delay times calculated from chemical kinetic modelling are presented alongside pressure-temperature trajectories of the in-cylinder gases to explain the trends. The underlying cause of the trends is explained by using a sensitivity analysis to determine the contribution of each reaction within the chemical kinetic mechanism to first-stage ignition, revealing the effect of introducing ethanol on the OH radical pool and resulting LTHR intensity.

Keywords: Low temperature heat release, ethanol, iso-octane

1. Introduction

The contribution to global CO_2 emissions from light-duty vehicles (LDVs) must be reduced as quickly and effectively as possible to mitigate the effect of climate change. At present, the vast majority of LDVs are propelled by the internal combustion engine (ICE) [1]. One route to reduced net CO_2 emissions from ICEs is the adoption of low-carbon and carbon-neutral fuels such as biofuels and e-fuels. Bioethanol is produced from biogenic matter and contains carbon originating from CO_2 absorbed from the atmosphere during photosynthesis. Its uptake is increasing due to its ability to aid decarbonisation from the existing vehicle fleet, for example in the UK where standard gasoline moved from E5 to E10 (i.e. 5 to 10% vol ethanol) in 2021. Despite its slightly lower energy density, ethanol is a suitable candidate for a drop-in fuel to replace or displace crude oil fractions thanks to its high octane rating and lower combustion temperatures—this allows for higher efficiency through the use of high compression ratios and optimised ignition timing, and reduced emissions [1, 2, 3].

Lean combustion, where the air-fuel ratio is weak of stoichiometric, has the potential to increase the efficiency of ICEs by 10-20% by improving the ratio of specific heats of the mixture and reducing wall heat losses [4]. However, the widespread adoption of lean operation in modern spark ignition (SI) engines has been inhibited by its associated challenges with ignition, combustion stability and compatibility with three-way catalysts to treat NO_x emissions. Problems with NO_x emissions have been mostly solved either with an advanced technique in-cylinder [5] or an on-board after-treatment system—which comes with an associated efficiency penalty. Ignition and combustion control issues are exaggerated during ultra-lean operation—a subset of lean operation where the equivalence ratio (ϕ) is (here defined as) less than 0.5 [6].

One potential remedy for the combustion control and ignition problems with lean mixtures is Low Temperature Heat Release (LTHR); this is the phenomenon in which some of the fuel-air mixture undergoes a slower, exothermic reaction at relatively lower temperatures, producing

*Corresponding Author
Email address: felix.leach@eng.ox.ac.uk (Felix C.P. Leach)

intermediate species prior to the main combustion event. These intermediate species may have different combustion characteristics to the original fuel, therefore harnessing and controlling the underlying reactions could be key to improving lean combustion. Low temperature heat release is in contrast to high-temperature heat release (HTHR) in the main combustion event—where the chemistry differs and far more energy is released. HTHR is required for practical engine applications of combustion, whether it be caused by the second stage of autoignition, or a positive ignition source such as a spark plug.

The source of LTHR is heat released from the first stage of two-stage autoignition, which is often associated with fuel blends that exhibit negative temperature coefficient (NTC) behaviour. A fuel mixture that exhibits NTC behaviour has a non-monotonically decreasing relationship between ignition delay time and mixture temperature at certain pressures. In certain temperature ranges (depending on fuel) mixture reactivity decreases due to unfavourable equilibrium rates of radical forming reactions, ultimately leading to an ignition delay time that increases with temperature [7].

Fuels that exhibit strong NTC behaviour include iso-octane (2,2,4-trimethylpentane) and n-heptane, the two components of the primary reference fuels (PRFs), which are used in the standard Research Octane Number and Motor Octane Number (RON and MON) tests [8, 9]. Alkane fuels, particularly straight-chained alkanes, are most likely to exhibit this behaviour, unlike alkenes and aromatics which have different low temperature chemistry [7, 10].

Unlike iso-octane and n-heptane, ethanol does not exhibit NTC behaviour and therefore does not exhibit two-stage autoignition, however, iso-octane ethanol blends of up to 20%vol ethanol have been shown to exhibit NTC behaviour in an Ignition Quality Tester [11]. In other studies, introducing ethanol into iso-octane blends in a homogeneous charge compression ignition (HCCI) engine running at 600 and 900 rpm was shown to reduce LTHR peaks [12]. Furthermore, ethanol has been observed to be more effective at radical scavenging than iso-octane [13].

The occurrence of LTHR in HCCI engines and gasoline compression ignition (GCI) engines has been well reported [14, 15, 16, 17]. In these engines, the occurrence of LTHR has been taken advantage of to control combustion heat release rate via partial fuel stratification [18]. Furthermore, LTHR has been studied in reactivity controlled compression ignition (RCCI)

engines, where the low temperature reactions can have an important role in curating varying degrees of charge reactivity and therefore help control high temperature heat release [19, 20, 21].

More recently, LTHR has been shown to also occur in SI engines, occurring before the spark under certain conditions—where it is termed pre-spark heat release (PSHR) [22]. The occurrence of LTHR has been found to make knock onset less sensitive to inlet temperature by moving the mixture's thermodynamic state into a long ignition delay (low reactivity) region [22]. In other circumstances, the frequency and intensity of low speed pre-ignition have been found to correlate with LTHR magnitude [23]. It has been hypothesised that LTHR-induced changes in mixture composition increase its laminar flame speed, which accelerates combustion [24], this could ultimately lead to improved combustion efficiency, particularly for ultra-lean operation where low flame speeds can be a limiting factor.

The effect of engine and mixture parameters on LTHR have been explored in previous studies [25, 26]:

- Increased inlet pressure generally encourages the occurrence of LTHR onset and increases its magnitude as higher pressures reduce ignition delay time.

- Increasing compression time by reducing engine speed increases the magnitude of heat release by LTHR, by allowing more time for chain-branching exothermic reactions to occur. Increasing the compression time too far allows the mixture sufficient time to progress to the second stage of two-stage autoignition, resulting in high temperature heat release.

- The effect of increasing engine inlet temperature and therefore compression temperature is non-linear and depends on many other factors. LTHR is more prominent with increasing temperature until the compression temperatures reach the NTC ignition delay region, at which point LTHR intensity decreases. The more time spent at temperatures corresponding to low first-stage ignition delay (usually defined by a 50K temperature rise), the more prominent LTHR is. Hence, increasing compression temperature can either increase or decrease the strength of LTHR, depending on the starting conditions.

- LTHR magnitude increases as equivalence ratio increases due to reactivity enhancement, up until a certain limit in direct injection engines, where the thermal cooling effects of fuelling overpower reactivity enhancement, and LTHR is abruptly quenched.

To date, much research on Low-Temperature Heat Release (LTHR) has predominantly centred around iso-octane and n-heptane, because they are the two components of PRFs. However, these compounds, with their pronounced NTC characteristics, do not comprehensively represent all elements of contemporary gasoline blends. Octane sensitivity defines the difference between RON and MON and therefore is implicitly tied to the NTC behaviour of iso-octane and n-heptane; fuels with the highest octane sensitivity have demonstrated superior performance in some tests, especially those mirroring modern engine conditions [27] where LTHR was also present. Consequently, there is a pressing need for a more nuanced understanding and quantification of fuel performance that takes into account modern engines and incorporates the effects of LTHR.

The chemistry of LTHR can be studied both experimentally, and computationally, via chemical kinetics simulations of engines and ignition delay times in software packages such as CHEMKIN.

In the past, investigating the effect on LTHR in SI engines, of variables such as those above or others such as fuel blends, has been challenging—pressure-derived heat release analysis techniques cannot distinguish between low temperature heat release and other concurrent sources of heat release, such as HTHR from deflagration. A recently developed technique [25] is employed in this work to investigate the effects of blending ethanol with iso-octane on the occurrence of low temperature heat release in isolation.

2. Methodology

2.1. Experimental Facility

The experimental investigations employed a single-cylinder, gasoline direct injection engine based on a Ricardo Hydra bottom end with technical specifications as detailed in Table 1. The engine was connected to a 57 kW AC motoring dynamometer (Vascat MAC-Q) that controlled speed ($\pm$1 rpm). Fuel injection settings including timing, duration and fuel rail pressure were controlled with a Schaeffler Protronic ECU using an ETAS INCA interface and the spark plug was

disabled. Intake pressure was maintained at desired levels using an external boosting rig, with the throttle kept wide open throughout. Intake air was heated using an electric heater installed upstream of the throttle. Engine coolant and oil temperatures were maintained at 90 °C.

Inlet temperature and pressure were measured around 350 mm upstream of the inlet ports using a Druck UNIK 5000 pressure sensor and a 3 mm type K thermocouple, respectively. The fuel flow rate was measured using a Coriolis (Siemens FC Mass 2100) and the air flow rate was measured with a hot wire (Sierra-CP Airtrak 628S) flow meter. Exhaust composition was measured with a Horiba MEXA-ONE emissions analyser. These parameters were recorded at 1 Hz using a Sierra-CP CADET system for 30 seconds per test. A water-cooled piezoelectric transducer (Kistler-6041B) was used to measure cylinder pressure at a resolution of 0.1 °CA using an AVL Indiset data acquisition system; these high-speed measurements were recorded for 300 cycles at a time. Data was post-processed with AVL Concerto and bespoke MATLAB scripts. Further details about the test cell can be found in previous publications [26, 28, 29].

Table 1: Engine specifications

Bore [mm]	83.0
Stroke [mm]	92.0
Displacement [cm^3]	500.0
Compression ratio	10.56:1
Fuel injection system	Production direct injector centrally mounted in cylinder head

2.2. Isolating LTHR

LTHR was induced by pressurising and heating the inlet air of the engine (which had SI geometry), as described in [25]. LTHR was isolated by disabling the spark, so as not to cause deflagration which would interfere with the heat release phenomena and intermediate species. Boosting, inlet heating and speed were monitored so as not to induce HTHR from the second stage of two-stage autoignition, in order to preserve the engine (and because HTHR is not of

interest for this study).

2.3. Operating Conditions

Tests were performed at a constant speed of 1500 rpm and inlet pressure of 1.5 bar (absolute). A broad range of inlet temperatures (40–140 °C) were tested, to maximise the compression temperature range explored by the fuel-air mixtures. Equivalence ratios of 0.5, 0.67 and 1.0 were chosen in order to investigate the behaviour at stoichiometric and lean conditions, where the consequences of LTHR chemistry are relevant.

Equivalence ratios were calculated from fuel and air flow measurements, and verified from exhaust emissions using the 'Spindt' method [30] up to $\phi \approx 0.55$. Beyond that, the exhaust unburned hydrocarbon sensor started to saturate and only the air and fuel flow measurements were used for determining ϕ. Inlet temperatures were maintained within ± 2 °C and pressure within ± 0.01 bar. Engine settings are listed in Table 2.

Table 2: Engine settings

IVO [°CA aTDC]	-352
IVC [°CA aTDC]	-165
EVO [°CA aTDC]	159
EVC [°CA aTDC]	359
Speed [rpm]	1500
Injection pressure [bar]	140
Injection timing [°CA aTDC]	-300
Inlet temperature [°C]	40, 60, 80, 100, 120, 140
Inlet pressure (P_{in}) [bar]	1.5
Equivalence ratio (ϕ)	0.5, 0.67, 1.0

2.4. Test fuels

Table 3 shows the four two-component test fuels that were blended from iso-octane and ethanol (both 99.5+ % purity). Fuels were coded (and will subsequently be referred to) using

"OE" and their %vol of ethanol: OE05 is 5% ethanol, for example. Blends simulated computationally followed the same rule, with the range of ethanol percentages extended. Blends above 20% ethanol were not studied as this was the detectable limit for LTHR in the conditions. The fuel system was manually drained and then flushed for 25 minutes between test runs with different fuels in order to avoid contamination.

Table 3: Test fuels

Fuel	**OE00**	**OE05**	**OE10**	**OE20**
Iso-octane [%vol]	100.0	95.0	90.0	80.0
Ethanol [%vol]	0.0	5.0	10.0	20.0
Ethanol [%mass]	0.0	5.7	11.3	22.2
Ethanol [%mol]	0.0	13.0	24.0	41.5

2.5. Quantifying LTHR

To quantify the amount of energy released from low temperature heat release, net apparent heat release rate (AHRR), $\frac{\mathrm{d}Q_\mathrm{n}}{\mathrm{d}\theta}$ (defined as the heat release rate $\frac{\mathrm{d}Q_\mathrm{hr}}{\mathrm{d}\theta}$ less the heat transfer rate $\frac{\mathrm{d}Q_\mathrm{ht}}{\mathrm{d}\theta}$) was calculated in MATLAB using the crank angle, θ, based pressure, p, and cylinder volume, V, (calculated from engine geometry) traces according to Equation 1 [31], using a constant ratio of specific heats $\gamma = 1.35$:

$$\frac{\mathrm{d}Q_\mathrm{n}}{\mathrm{d}\theta} = \frac{\mathrm{d}Q_\mathrm{hr}}{\mathrm{d}\theta} - \frac{\mathrm{d}Q_\mathrm{ht}}{\mathrm{d}\theta} = \frac{\gamma}{\gamma-1} p \frac{\mathrm{d}V}{\mathrm{d}\theta} + \frac{1}{\gamma-1} V \frac{\mathrm{d}p}{\mathrm{d}\theta} \tag{1}$$

To distinguish heat release Q_hr measurements originating from isolated LTHR from heat transfer Q_ht effects and other assumptions, the calculated AHRR trace for a corresponding unfuelled, motored case was subtracted from the fuelled case. The start and end of LTHR were determined by finding points around top dead centre (TDC) where the AHRR of the fuelled case (with motoring case subtracted) deviated from zero. The isolated LTHR methodology (as introduced by White et al [25]) meant that no HTHR was present and hence any heat release from the calculated trace was deemed to be LTHR. The AHRR was then integrated between the start and end boundaries to find the total heat release in Joules per cycle.

Cylinder temperature was calculated using the ideal gas law with measurements of cylinder pressure, cylinder volume and estimations of cylinder contents.

2.6. Chemical Kinetics Modelling and Sensitivity Analysis

Ignition delay simulations were performed in CHEMKIN using the closed homogeneous ignition delay model with a constant volume. The simulations modelled reactions for 200 ms, and reported ignition delay defined by a 50 K rise in temperature, in order to detect the relatively small rises in temperature caused by LTHR, as in [22, 27]. Mixtures of air and iso-octane were modelled at $\phi = 0.5$ and $\phi = 1.0$ using a reduced Lawrence Livermore National Laboratory (LLNL) gasoline surrogate mechanism with 165 species and 839 reactions [32]. The contribution of each reaction within the mechanism to LTHR was determined by performing a brute force sensitivity analysis, modifying the rate constant, k, of each reaction in turn and determining the subsequent effect on ignition delay time, τ. The sensitivity coefficient, S, was calculated using Equation 2 [33], where the $+$ and $-$ subscripts correspond to the cases with increased and decreased rate constants respectively. The simulations were run in CHEMKIN, controlled by a version of Pysens [34], modified to run on Windows 10.

$$S = \frac{\log_{10}(\tau_+/\tau_-)}{\log_{10}(k_+/k_-)} \tag{2}$$

2.7. CO as an indicator of LTHR

Before discussing the effect of ethanol content on low temperature heat release, the most effective metric for quantifying LTHR was determined. Traditionally, pressure-derived apparent heat release methods (as described in section 2.5) have been used, and often lead to satisfactory estimates when test points are similar and LTHR is strong. However, when thermal effects are significant and LTHR is weak (but present), this method ceases to give perfectly accurate measurements. This is because heat transfer effects are not fully ruled out and the precise methodology regarding the start and end of LTHR can be subjective.

Reactions involved in LTHR lead to the formation of carbon monoxide (CO), and hence the extent to which CO is present in exhaust gasses has been shown to provide a good, proportional,

proxy for the intensity of LTHR when using the isolated LTHR methodology [26]; note that this is not the case when HTHR occurs alongside or after LTHR as the CO will be oxidised during complete combustion.

Figure 1, which shows direct exhaust CO measurements against estimated heat release using the pressure-derived method demonstrates the issue. It is particularly noticeable in the fuels with higher ethanol content. In fact, test points that showed no signs of LTHR (such as some OE10 test points and all OE20 test points) led to erroneous readings of over 20 Joules. These readings are a result of differences in apparent heat release traces between pure air and the non-reacting air-fuel mixture, which stem from thermodynamic properties of mixtures, such as heat capacities, and differing initial temperatures stemming from charge cooling.

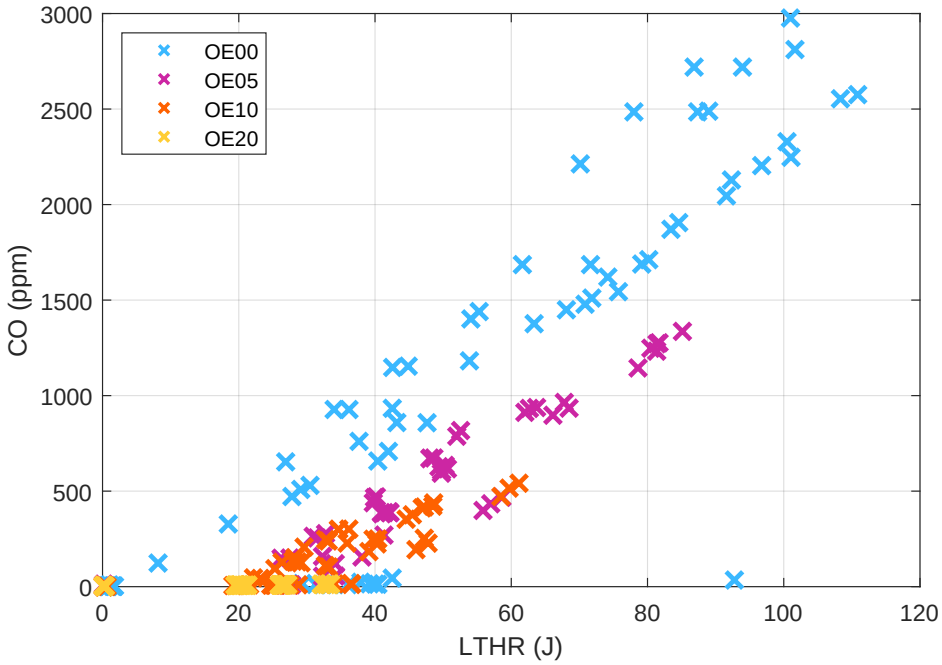

Figure 1: Exhaust carbon monoxide measurements versus total heat released by LTHR according to the pressure-based methodology described in [25], for all fuels and inlet temperatures

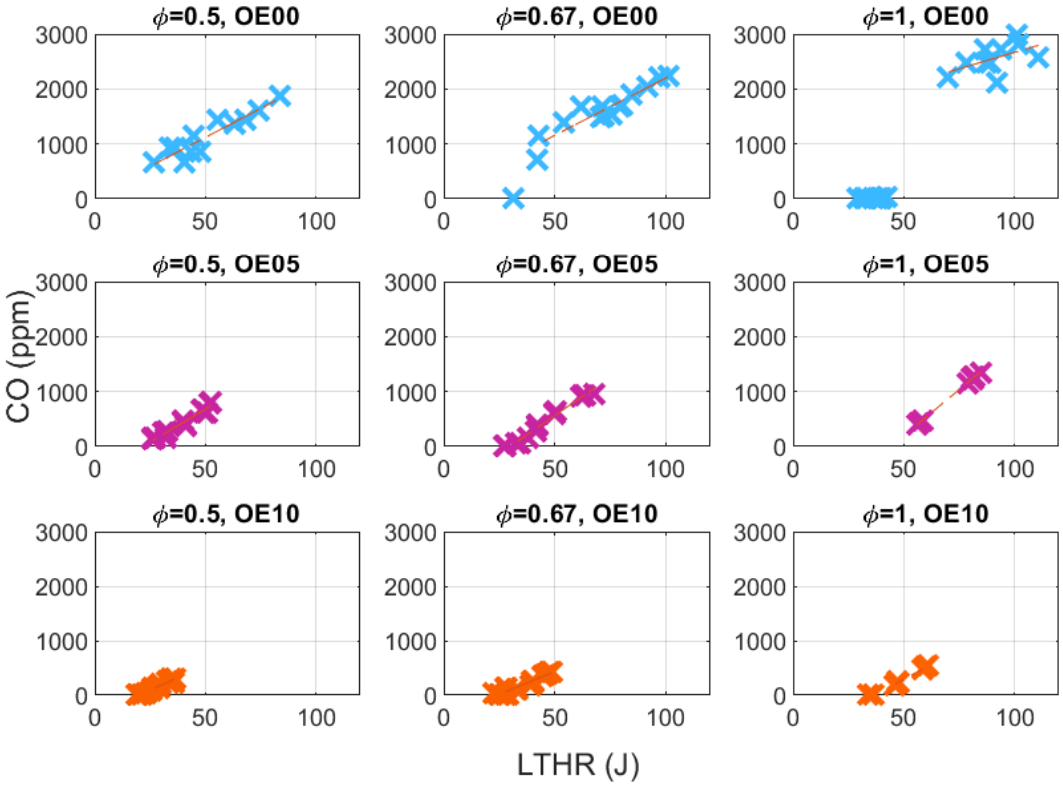

Figure 2: Demonstration of the linear relationship between exhaust carbon monoxide measurements and total heat released by LTHR (according to the pressure-based methodology), grouped up by equivalence ratio and test fuel for OE00, OE05 and OE10

In fact, the linear CO-LTHR relationship that is typically observed can also be seen in this data, once it is split up into separate fuel and equivalence ratio groups. Figure 2 shows this, with the constant offset-measurement error in LTHR-for the various combinations; OE20 is omitted as no signs of LTHR were measured. The likely cause of this constant overestimation in pressure-derived LTHR measurement is explained above. This overestimate also applied to OE00 points (at $\phi = 0.67$ and $\phi = 1.0$) that didn't experience any LTHR, hence they were not included in the linear fitting process.

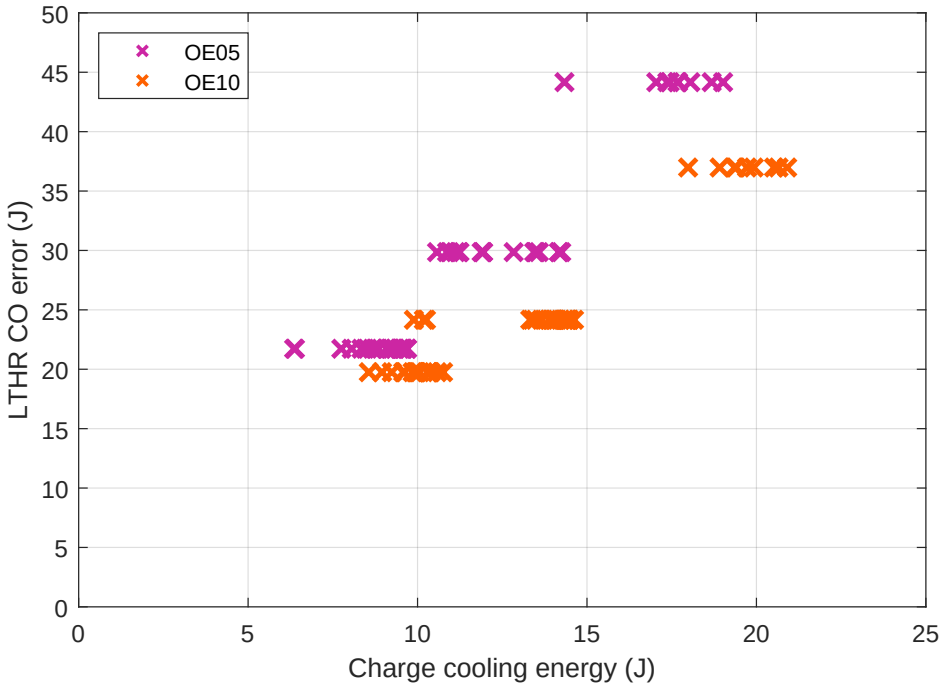

Figure 3: The measurement error of the thermodynamic LTHR quantifying methodology (as implied by linear CO measurements) plotted against calculated charge cooling energy for OE05 and OE10 test points

When this error (the x-intercept for each fuel-equivlance ratio combination in Figure 2) is plotted against the energy "lost" to charge cooling (which itself is a function of fuel and equivalence ratio) an approximate doubling trend is observed (Figure 3). Charge cooling energy was calculated by multiplying the measured mass of fuel injected by the enthalpy of vaporisation, using data from [35]. This did not apply to the pure iso-octane data set, where the error was minimal (0 to -5J)—apart from the stoichiometric case where increased uncertainty in the pressured-derived measurements stopped the correction method from working effectively.

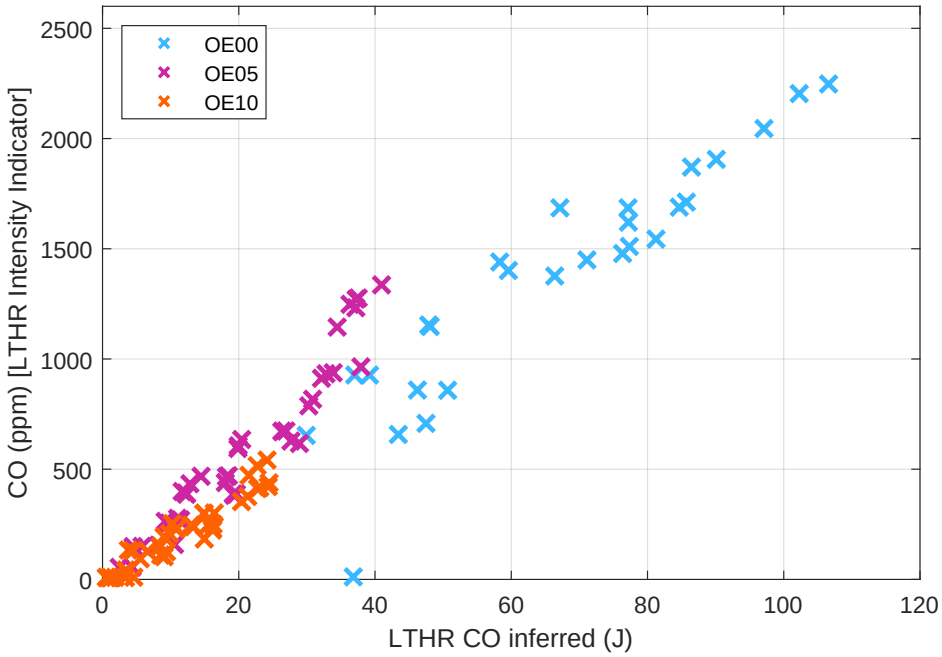

Figure 4: Exhaust carbon monoxide measurements versus total heat released by LTHR according to the pressure-based methodology described—incorporating a correction offset, for all test points

The effect of this correction is shown in Figure 4 and serves to demonstrate that carbon monoxide is a more effective indicator for LTHR intensity in this work.

3. Results

3.1. Effect of ethanol on measured LTHR intensity

Figure 5 shows an overview of the experimental results at all the conditions tested. LTHR behaviour of iso-octane is consistent with trends in the literature; at the low equivalence ratio point, LTHR occurred at all inlet temperatures, with the lower inlet temperatures proving favourable. As the equivalence ratio increased to 0.67, LTHR ceased at the lowest inlet temperature and peaked around $T_{in} = 80$ °C. The inlet temperature for which LTHR ceased decreased to around $T_{in} = 60$ °C for the stoichiometric case. This relatively sudden cutoff has been attributed to the effect of charge cooling on the pressure-temperature history and therefore autoignition chemistry of fuel-air mixtures [6].

OE05 displays a similar trend to iso-octane, albeit with only around half the LTHR intensity; the LTHR peak also occurs at higher temperatures–the precise reason for this will be explained

in section 3.3. OE10 continues this trend, with increasing inlet temperatures for maximum LTHR intensity, with approximately half the LTHR occurring as indicated by the exhaust CO.

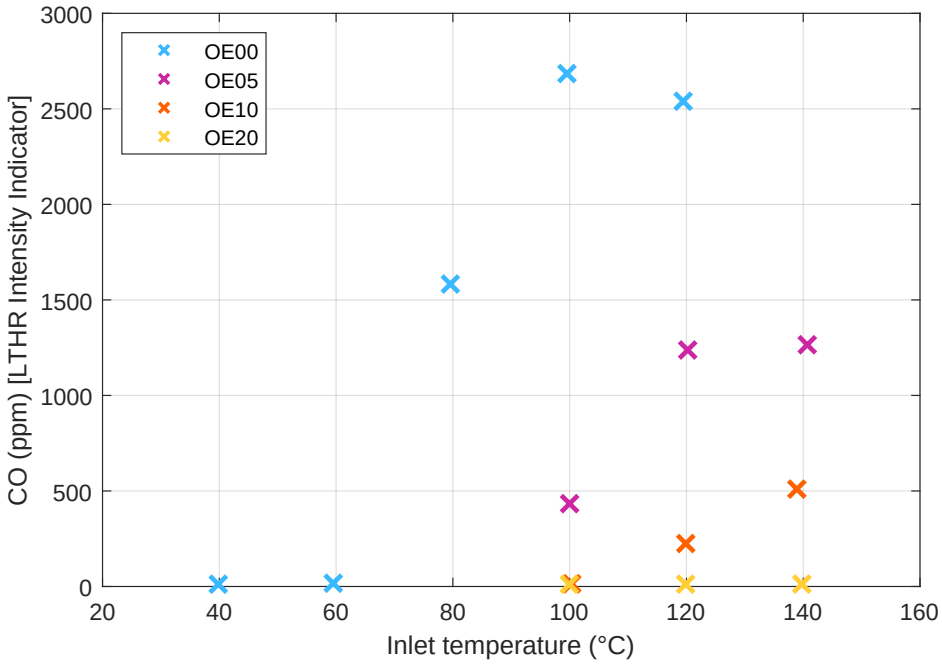

(a) $\phi = 1$

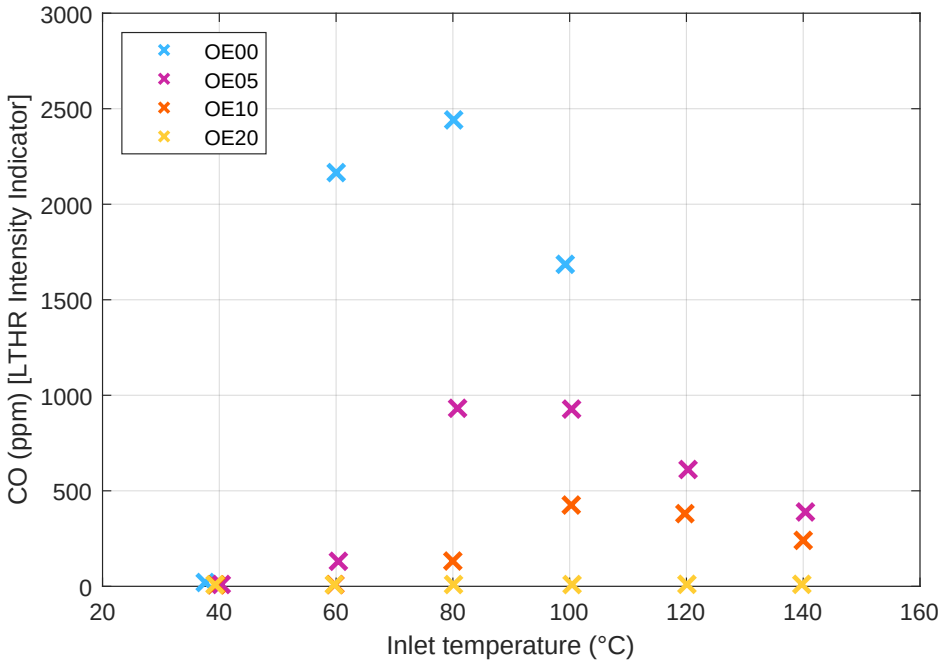

(b) $\phi = 0.67$

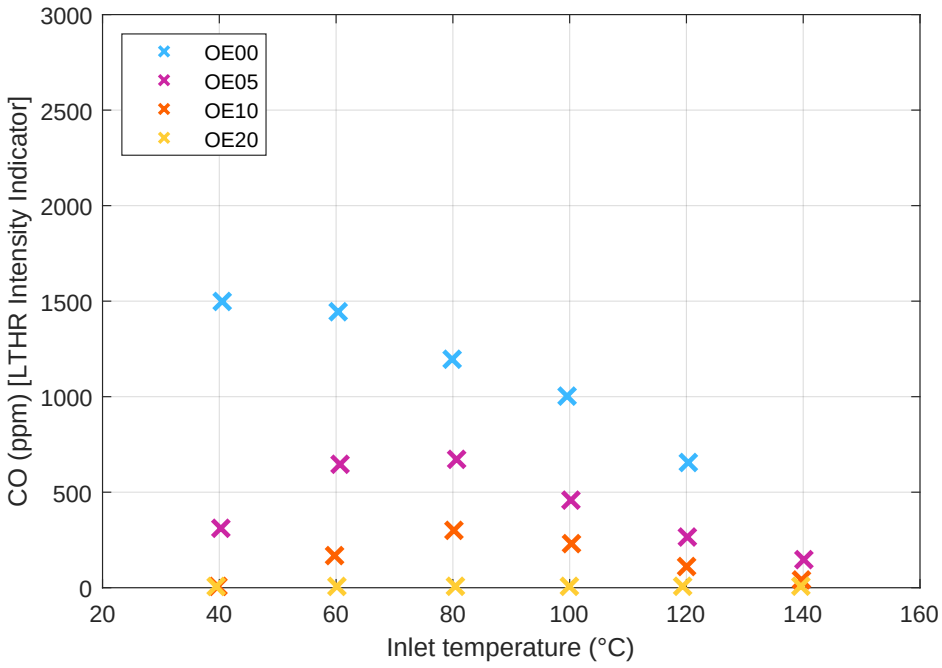

(c) $\phi = 0.5$

Figure 5: Exhaust CO concentration (as a proxy for LTHR intensity) plotted for different fuels inlet temperatures and equivalence ratios

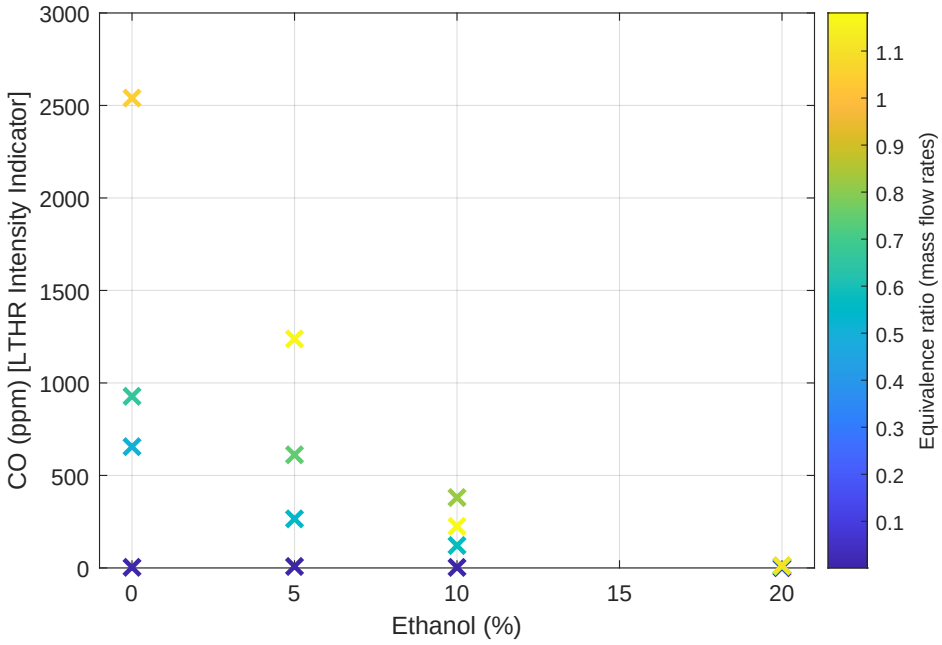

Figure 6: Exhaust CO concentration plotted against fuel ethanol content (%vol) for $T_{in} = 120$ °C

Increasing the ethanol content in the fuel always decreased the amount of LTHR observed for every test point; this trend can clearly be seen in Figures 6 and 7. $\phi = 0.5$ and $T_{in} = 120$ °C were chosen for plotting as they contained the most data points and the trends observed are representative of all data that was collected. OE20 displayed no signs of LTHR for any combination of inlet temperature or equivalence ratio. The results are stark—the reduction in low temperature heat release is far greater than can be accounted for by the displacement of iso-octane with a non-LTHR-exhibiting fuel in the blend. Instead, the observed behaviour must be accounted for by chemical and physical effects resulting from the introduction of ethanol into the iso-octane blends.

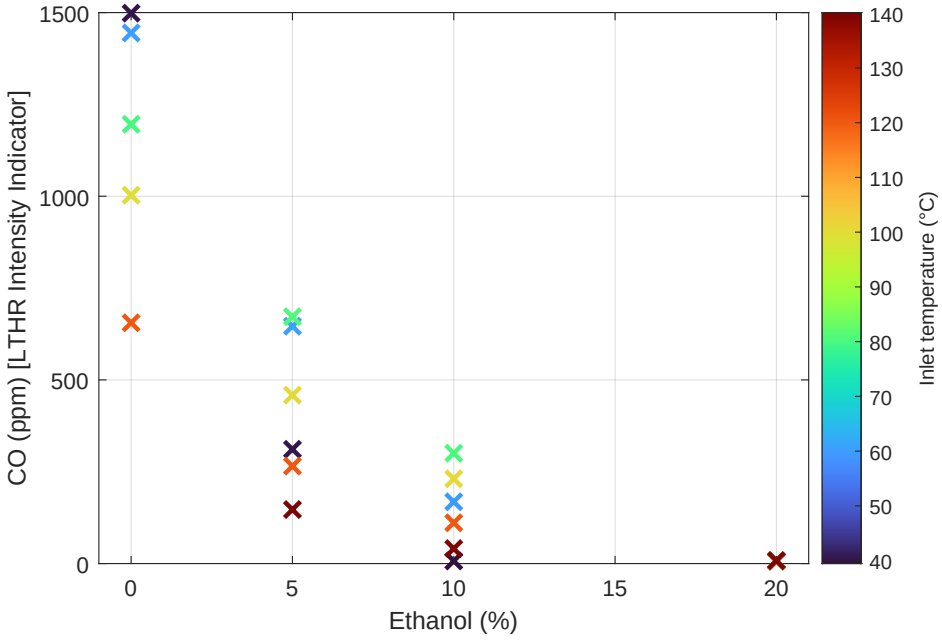

Figure 7: Exhaust CO concentration plotted against fuel ethanol content (%vol) for $\phi = 0.5$

3.2. Effect of Ethanol on LTHR phasing

Increasing ethanol content was found to retard the phasing of LTHR, as shown in Figure 8; a 10% vol increase in ethanol content delayed the CA50 of low temperature heat release by as much as 15 °CA. $\phi = 0.5$ has been shown here as it contained the most data points at different operating conditions; the other equivalence ratios exhibited the same trends. The first stage ignition delay times for these blends are of the same order of magnitude of the time the mixtures spend at elevated

cylinder pressures and temperatures, hence LTHR phasing is dependent on ignition delay time and engine speed. Increasing ethanol content in the blend increases first stage ignition delay time, hence LTHR occurs later for the higher ethanol blends.

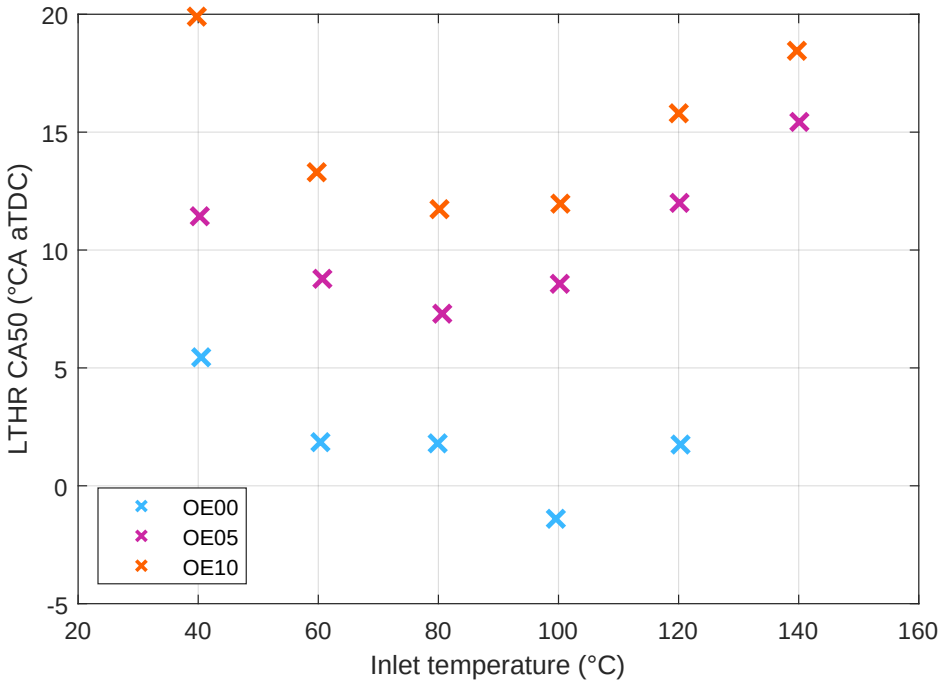

Figure 8: LTHR CA50 plotted for different fuels and inlet temperatures at $\phi = 0.5$

Comparison of Figures 5c and 8 suggest a strong relationship between LTHR intensity and phasing, which is confirmed in Figure 9. LTHR is too slow and commencing too late for high ethanol blends. This also explains the advancing-then-retarding nature of the phasing as inlet temperature increases.

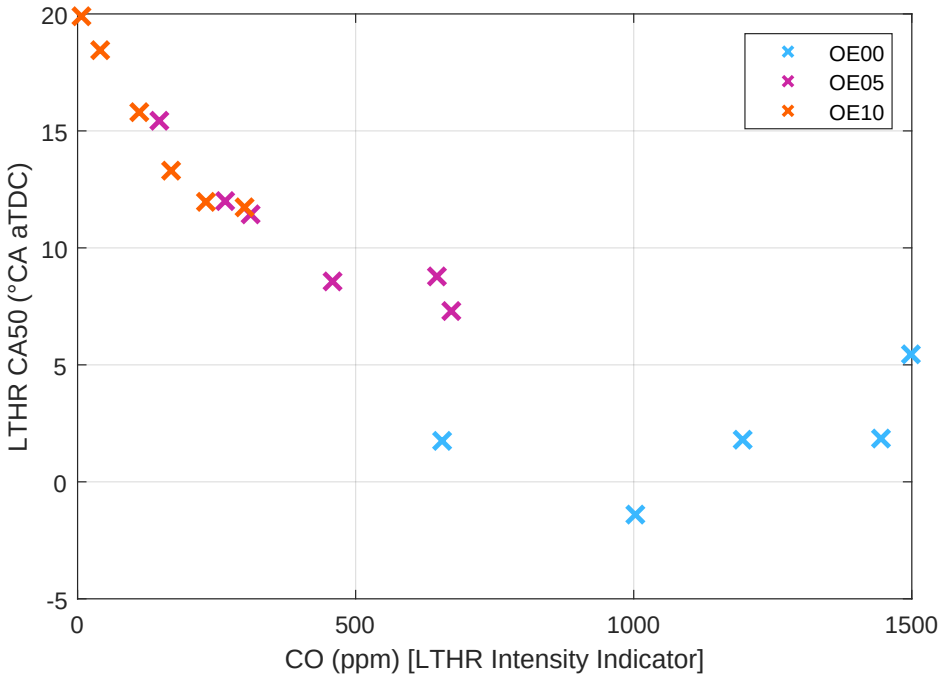

Figure 9: LTHR CA50 plotted against exhaust CO concentration at $\phi = 0.5$

3.3. Ignition delay analysis

Low temperature heat release originates from the heat released by fuels during the first stage of autoignition, so ignition delay simulations can be combined into an ignition delay contour, which represents how reactive (with respect to LTHR) a given fuel-air mixture is at different temperatures and pressures. The rate of progress towards first stage autoignition depends on the current thermodynamic state of a mixture—this changes rapidly in a motoring engine, but in general, the further a mixture progresses into the short ignition delay region—and the more time it spends there—the more progress can be made towards first stage autoignition and the more heat will be released by LTHR. In this section, specific cases for different fuels at a range of equivalence ratios are analysed.

The OE00 trends observed in Figure 5a can be further explained by analysing the pressure-temperature trajectories (from inlet valve closing to 10 °aTDC) in Figure 10, which are overlaid onto an ignition delay contour of OE00 at $\phi = 1.0$. In these plots, the temperature and pressure axes refer to both the temperature (and pressure) of the experimental data (in the pressure-temperature trajectories) and the initial temperature (and pressure) for each ignition delay simulation. The

three higher temperature cases penetrate the LTHR region—the pressure-temperature space with relatively short ignition delays. The effect of heat released from LTHR can be seen directly in the trajectories—there is a sharp temperature increase at around 32 bar, caused by the temperature rise associated with LTHR. The T_{in} = 100 °C and T_{in} = 120 °C cases traverse the regions with the shortest ignition delay, explaining why these points exhibited the greatest LTHR intensity in Figure 5a.

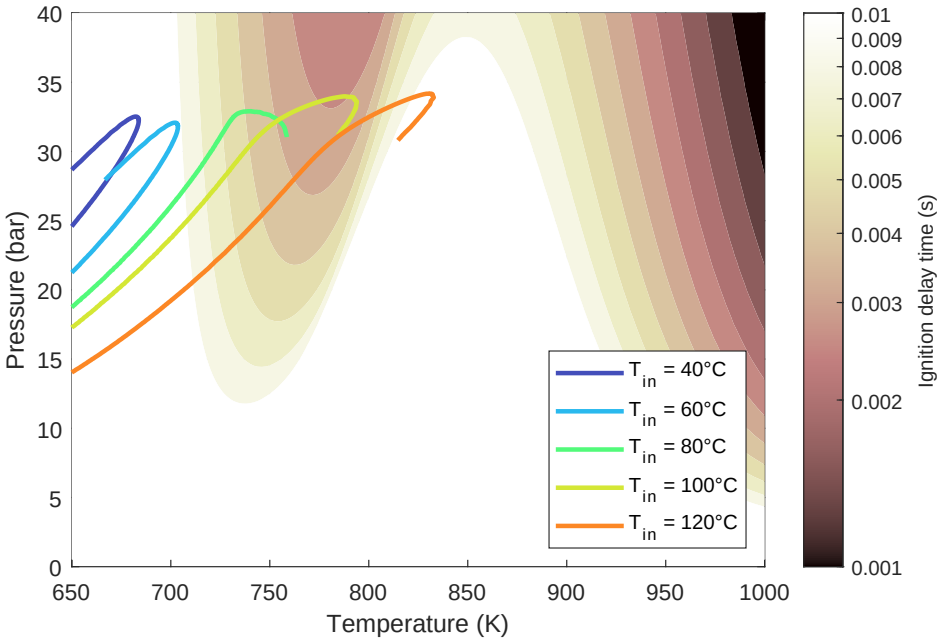

Figure 10: Pressure temperature trajectories for OE00 test points with varying inlet temperatures from T_{in} = 40 °C to T_{in} = 120 °C, superimposed onto an ignition delay contour (defined by a 50 K rise in temperature) for OE00 at $\phi = 1$

Similarly, the OE05 trends observed in Figure 5c can be explained by analysing Figure 11, which shows cylinder pressure-temperature trajectories overlaid onto an ignition delay contour of OE05 at $\phi = 0.5$. The trajectories corresponding to inlet temperatures of T_{in} = 60 °C and T_{in} = 80 °C traverse the region with the shortest ignition delay, i.e. the most reactive low temperature region—this explains why the T_{in} = 60 °C and T_{in} = 80 °C cases exhibited the greatest LTHR for OE05 at this equivalence ratio. The effect of the heat release from LTHR can be observed in the trajectories directly: the T_{in} = 40 °C and T_{in} = 100 °C and greater cases display a "hooking" shape, where cylinder temperature is lower after TDC than it was at the

corresponding compression pressure due to heat transfer losses. Meanwhile, the $T_{in} = 60$ °C and $T_{in} = 80$ °C cases approximately trace back on themselves, suggesting that the heat released by LTHR approximately balances heat losses to heat transfer at the walls.

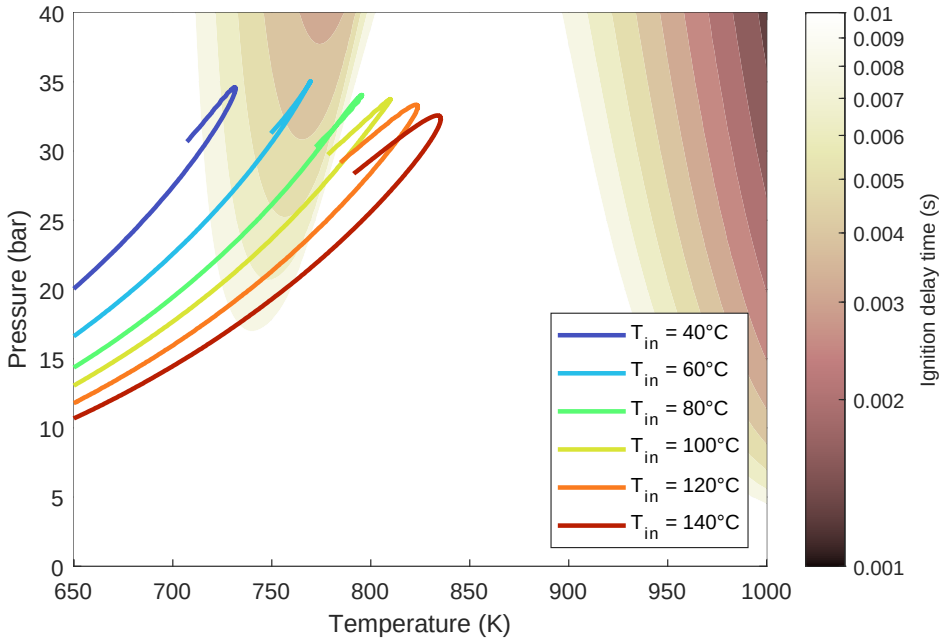

Figure 11: Pressure temperature trajectories for OE05 test points with varying inlet temperatures from $T_{in} = 40$ °C to $T_{in} = 140$ °C, superimposed onto an ignition delay contour (defined by a 50 K rise in temperature) for OE05 at $\phi = 0.5$

In Figure 12 the three trajectories 100 °C, 120 °C and 140 °C increase their penetration into the LTHR region with increasing inlet temperature. LTHR is only observed for the two highest inlet temperature cases for OE10 in Figure 5a, which is consistent with these trajectories.

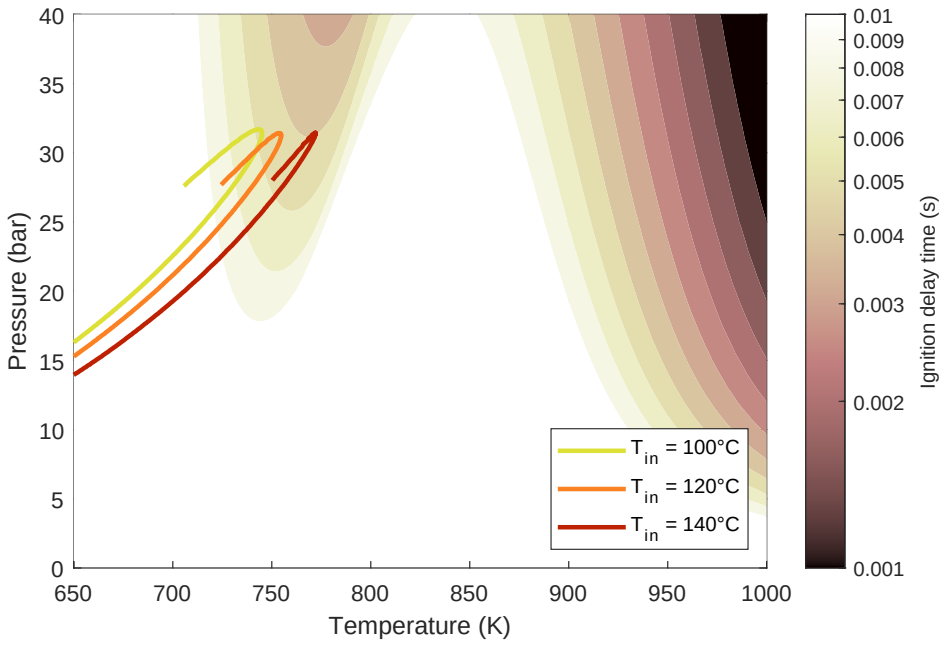

Figure 12: Pressure temperature trajectories for OE10 test points with varying inlet temperatures from $T_{in} = 100$ °C to $T_{in} = 140$ °C, superimposed onto an ignition delay contour (defined by a 50 K rise in temperature) for OE10 at $\phi = 1$

The pressure-temperature trajectories for OE20 all show the hooking behaviour consistent with non-reacting cases. The ignition delay contour for OE20 lacks the large LTHR region displayed by the lower ethanol content fuels and hence none of the trajectories reach regions where the ignition delay is less than 0.01s; the lack of LTHR observed in Figure 5c is not surprising.

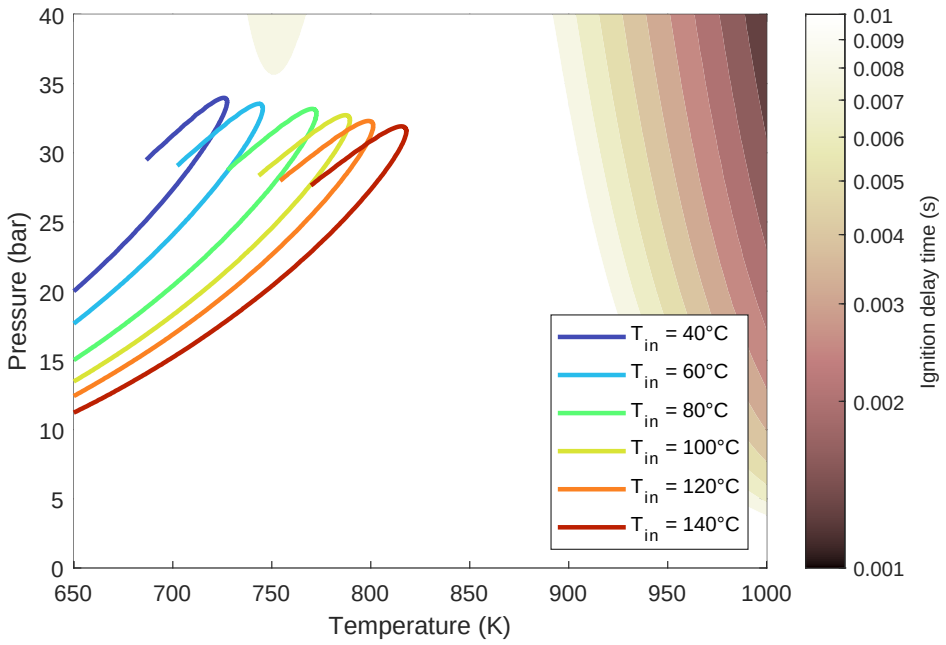

Figure 13: Pressure temperature trajectories for OE20 test points with varying inlet temperatures from $T_{in} = 40$ °C to $T_{in} = 140$ °C, superimposed onto an ignition delay contour (defined by a 50 K rise in temperature) for OE20 at $\phi = 0.5$

To compare the reactivity and thermodynamic differences in the fuels directly, pressure-temperature trajectories of the four fuel blends are shown in Figure 14; a (dashed) line of constant ignition delay (10 ms) is also plotted for each fuel to compare their reactivity. 10 ms was chosen as it corresponds to 90 °CA at 1500 rpm—i.e. 45 °CA either side of TDC, where pressures and temperatures are raised. The dashed lines show the decrease in reactivity as ethanol content increases, with the 10 ms line for OE20 being out of reach of the pressure-temperature trajectory at $T_{in} = 80C$ °C, $\phi = 0.5$. The trends shown at these inlet conditions are representative of the full dataset.

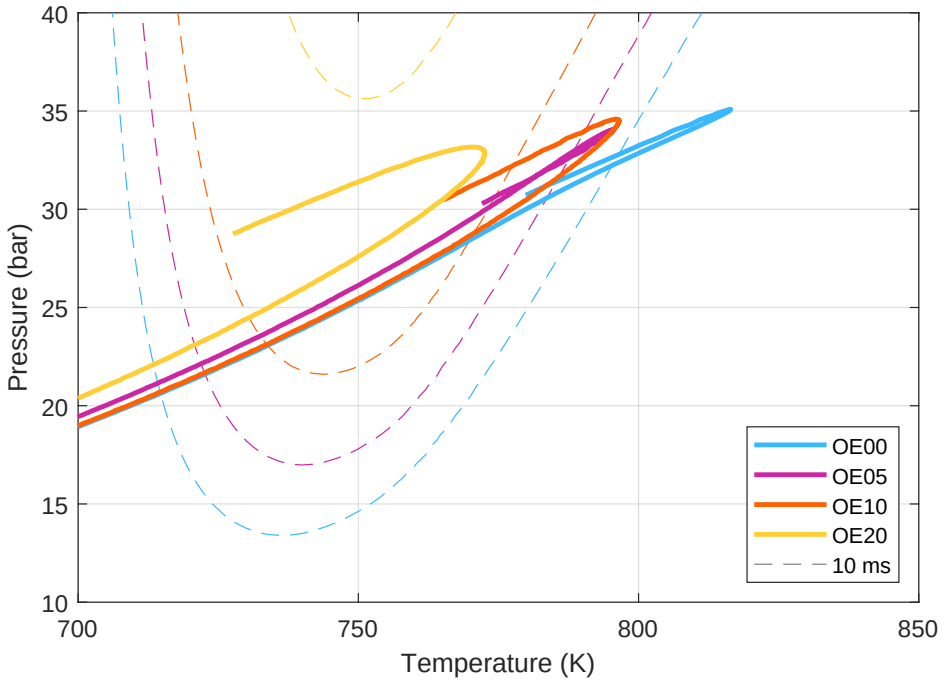

(a) $T_{in} = 80$řC at $\phi = 0.5$

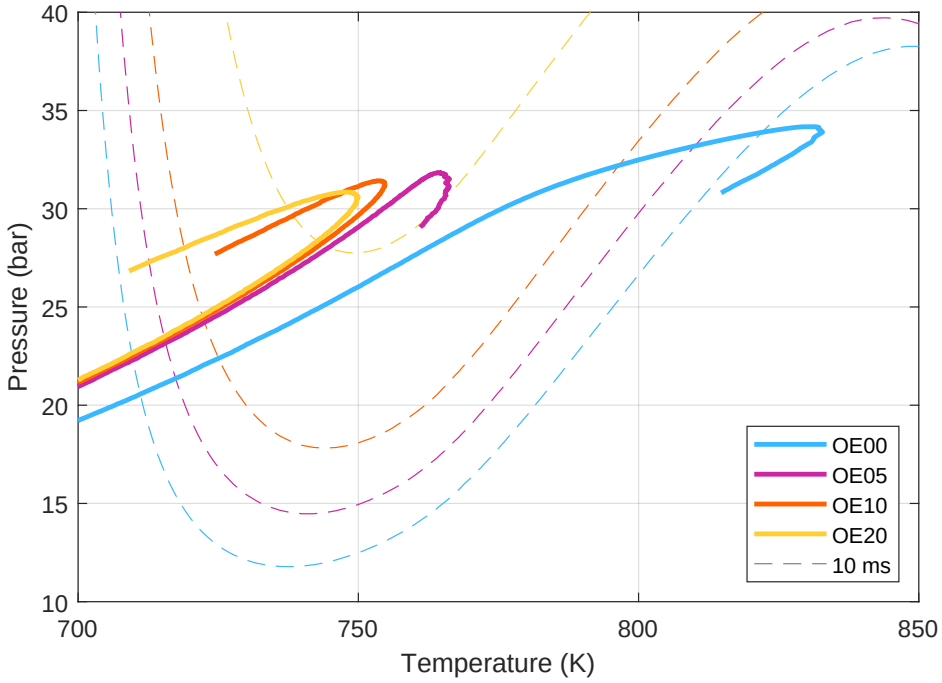

(b) $T_{in} = 120$ °C at $\phi = 1$

Figure 14: Pressure temperature trajectories of test points for each fuel, displayed on top of corresponding dashed lines of constant ignition delay of 10ms

The effects of charge cooling (which increases with ethanol content) can be seen in Figure 14a with the trajectories of the high ethanol fuels coming in at slightly reduced temperatures, though this behaviour is not entirely consistent and its effect is smaller than the reactivity differences, with a decreasing fraction of each fuel's pressure-temperature trajectory residing in the sub-10 ms region as ethanol content increases. Comparing the two sets of inlet conditions showed that the effect of ethanol at $T_{in} = 120$ °C at $\phi = 1$ seemed to be more significant. This is because, despite the high inlet temperature, the charge cooling associated with more mass injected reduces temperatures overall throughout the cycle, giving only the lowest ethanol blends the opportunity to undergo first stage autoignition.

Whilst the above plots show which parts of the LTHR region the pressure-temperature trajectories interact with, they do not directly measure time resided in these regions. In a system where the thermodynamic conditions and therefore the ignition delay is non-constant, the Livengood-Wu (LW) integral (Equation 3) can be used to quantify progress towards the continuously changing target of ignition delay time for a given fuel-air mixture.

$$\mathrm{LW} = \int_0^t \frac{dt}{\tau\left(T\left(t\right), P\left(t\right)\right)} \tag{3}$$

Figure 15 shows a scatter plot of the evaluation of this integral between the times corresponding to intake valve closing (IVC) and exhaust valve opening (EVO), against the measured exhaust CO concentration. A value of unity corresponds to the mixture reaching its first stage ignition delay on average, and the plot shows that all data points with a LW score of greater than one show significant LTHR intensity—in fact, every point with a score above 0.6 shows some LTHR as indicated by CO. Conversely, points with a score of less than 0.4 show little-to no LTHR behaviour. It is not entirely surprising that test cases with scores between 0.6 and 1 show some LTHR behaviour; this can be attributed to two reasons: slight inhomogeneities in-cylinder temperatures and equivalence ratios, and more importantly, the fact that some heat is released prior to reaching the peak of first stage autoignition.

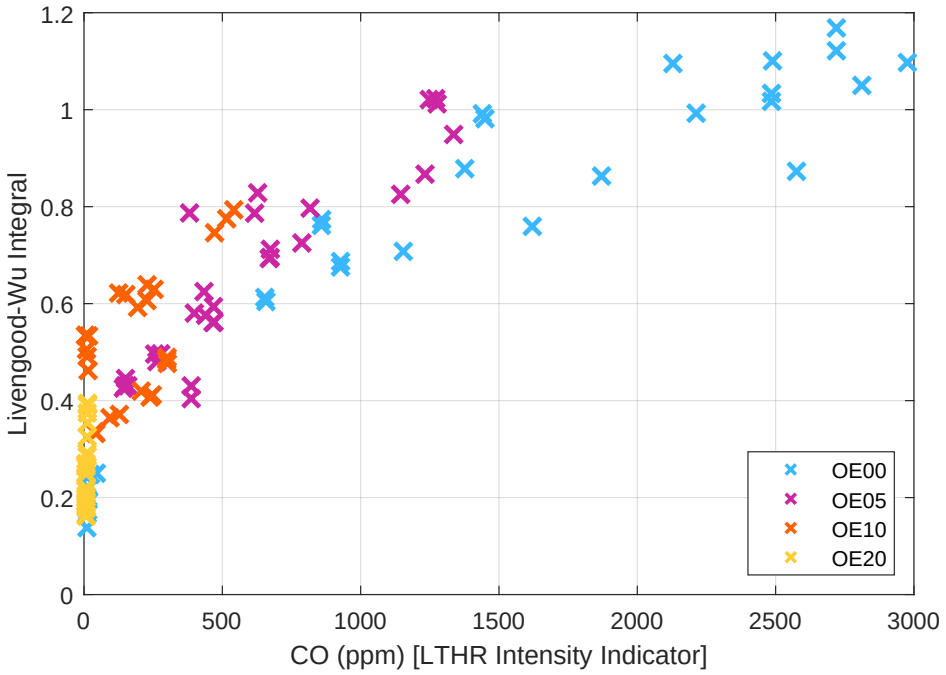

Figure 15: Ignition delay progress, as calculated by the Livengood-Wu integral between IVC and EVO, plotted against exhaust CO concentration

Figure 16 shows an example time series of temperature during an ignition delay simulation. For OE00 to OE10, two distinct rises in temperature are clearly seen. For maximum LTHR intensity, it is necessary to move the thermodynamic stage of a mixture into a region with very short first-stage ignition delay—however, the second-stage ignition delay (defined by the steepest rise in temperature) must also be relatively long, to minimise the chances of the LTHR developing into undesirable HTHR, such as in White et al.[25].

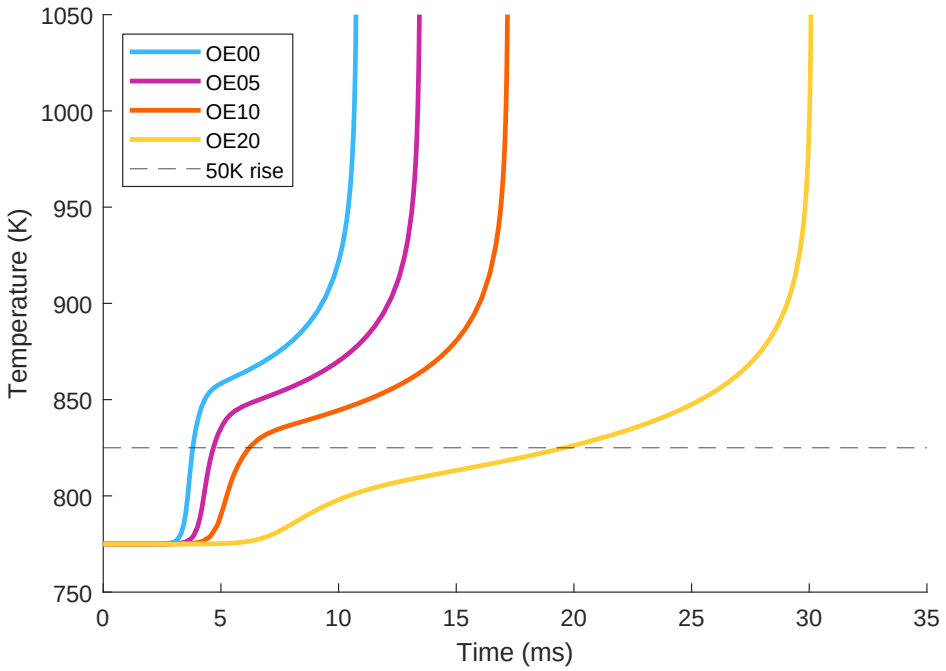

Figure 16: Ignition delay time series simulations for the four fuels in a constant volume reactor with $T_0 = 775$ °C and $P_0 = 28$ bar

The regions of pressure-temperature space where the difference between first stage and second stage ignition delay are greatest (but first stage is still short enough for LTHR to occur in engine timescales) are shown in Figure 17; the key region for LTHR in OE00 is 760–800 K, 26–33 bar, which is chosen for further exploration with an ignition delay time (brute force) sensitivity analysis.

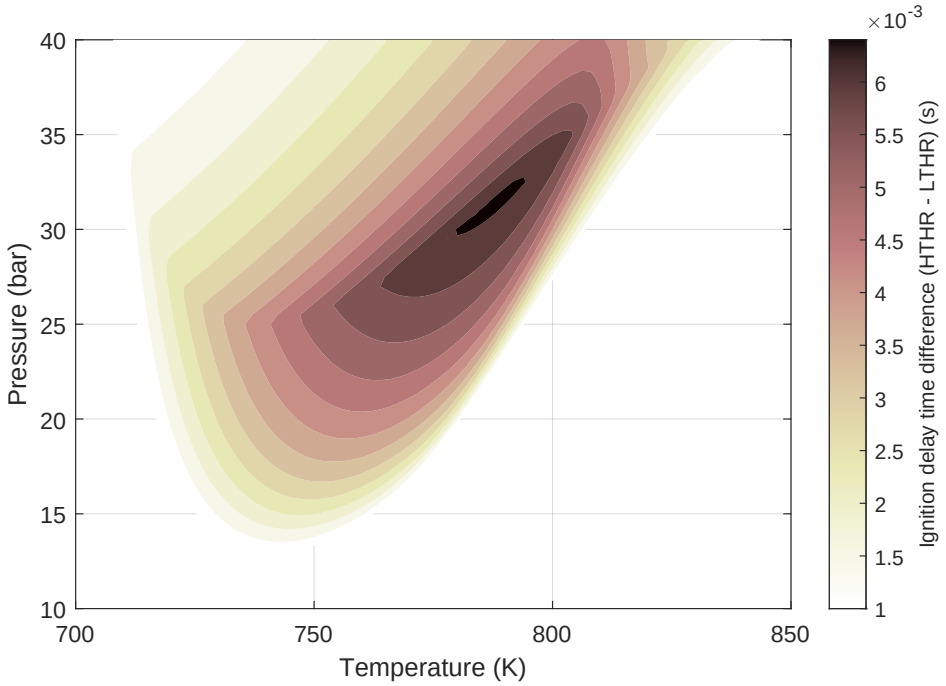

Figure 17: A contour showing the difference between first and second stage ignition delay time for OE00 at $\phi = 1$

3.4. Chemical Mechanism Analysis

A sensitivity analysis can be used to explain the fundamental cause of the results seen in this work. The most sensitive reactions are shown in Figure 18. A positive sensitivity coefficient means increasing the reaction rate increases the ignition delay time, which is not conducive to LTHR. Meanwhile, a negative sensitivity coefficient means that increasing reaction rate leads to a shorter wait for a 50 K rise, hence making a positive contribution to the occurrence of LTHR.

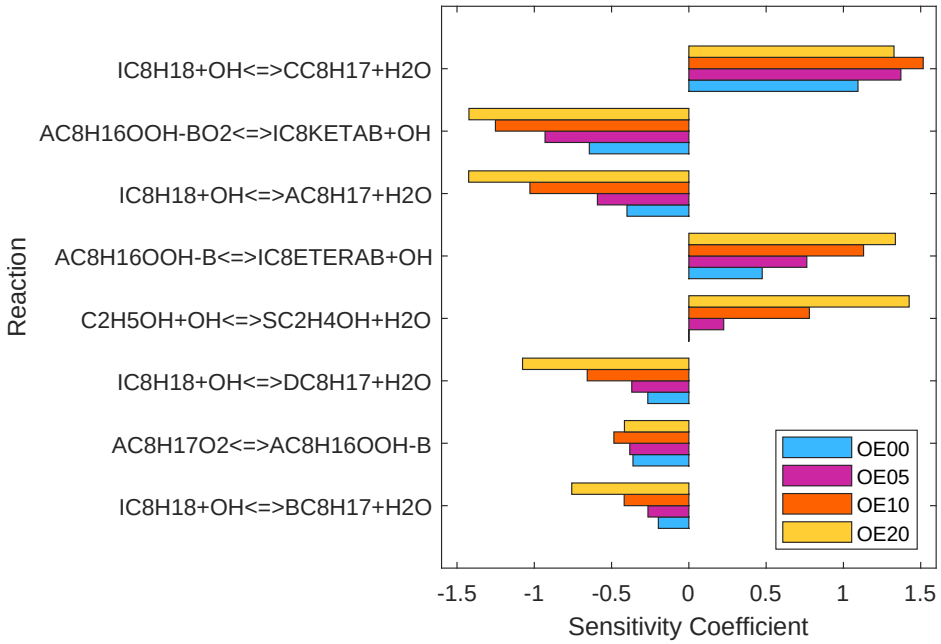

Figure 18: Sensitivity coefficients for the sensitivity of ignition delay time (by 50K rise) to reactions in the chemical kinetics mechanism that was used to simulate the four fuels in a constant volume reactor with $T_0 = 775$ °C and $P_0 = 28$bar

The four equations for hydrogen abstraction from iso-octane by a hydroxyl radical (reaction R1) are among the reactions with the highest sensitivity coefficients (appearing first, third, sixth and eight from the top in Figure 18):

$$\mathrm{iC_8H_{18} + OH \Longleftrightarrow xC_8H_{17} + H_2O} \tag{R1}$$

The x represents the four distinct sites for hydrogen abstraction. A and D are the 1° carbon atoms (1st and 5th along the chain, respectively), B corresponds to the 2° carbon atom and C represents the 3° carbon atom.

Reaction R2, hydrogen abstraction from ethanol (fifth from the top) also has a large sensitivity coefficient:

$$\mathrm{C_2H_5OH + OH \Longleftrightarrow sC_2H_4OH + H_2O} \tag{R2}$$

Reaction R3 (second from the top of Figure 18) forms an OH radical alongside a carbonyl-hydroperoxide molecule form the isomerisation of the peroxy-alkylhydroperoxide

(O_2QOOH) radical [36]; It is known to have a strong negative sensitivity due to its involvement in the low temperature chain branching process—the carbonyl-hydroperoxide molecule subsequently decomposes to the form a carbonyl radical and a second OH radical, i.e. two radicals from a stable molecule.

$$aC_8H_{16}OOH-bO_2 \Longleftrightarrow iC_8ketab + OH \tag{R3}$$

Meanwhile, reaction R4 (fourth from top), the decomposition of an hydroperoxyalkyl radical (QOOH) to a cyclic ether and OH radical is known to have a strong positive sensitivity coefficient because it does not promote the route to chain branching reactions such as reaction R3 [36].

$$aC_8H_{16}OOH-b \Longleftrightarrow iC_8eterab + OH \tag{R4}$$

Reaction R5 (seventh from top), alkylperoxy radical isomerisation to a hydroperoxyalkyl radical ($RO_2 \Longleftrightarrow$ QOOH), does not directly involve OH radicals, but is a precursor to reaction R3 and the subsequent chain branching and hence has a strong negative sensitivity coefficient [36].

$$aC_8H_{17}O_2 \Longleftrightarrow aC_8H_{16}OOH-b \tag{R5}$$

As ethanol content in the fuel increases, the positive sensitivity of hydrogen abstraction from ethanol (reaction R2) increases; meanwhile the negative sensitivities of the hydrogen abstraction of iso-octane by OH reactions increase (reaction R1), alongside reaction R3. This suggests that there is competition for the OH radical and that by introducing ethanol into the fuel blend, the OH radical pool is reduced, slowing down the low temperature reactions (as evidenced by their increasing ignition delay times) until ultimately they are longer than the time fuel-air mixtures spent at high compression temperatures and pressures, resulting in the observed behaviour of LTHR being strongly inhibited in the motoring engine.

The C version of the hydrogen abstraction from iso-octane by a hydroxyl radical (reaction R1) had a significant positive sensitivity but did not show a significant effect of ethanol ratio. This is in contrast with the three other hydrogen abstraction reactions which had negative sensitivity coefficients that increased with ethanol content. The site of initial hydrogen abstraction has implications further on in the low temperature oxidation of iso-octane; in the

absence of any ethanol, the four sites are effectively in competition with each other for OH radicals. The C-type reaction involves an internal carbon, and some of the subsequent reactions, such as alkyl radical decomposition (reaction type 3 in reference [36]) have a higher activation energy than for A, B and D type reactions, which is less conducive to LTHR—but not dependent on the presence of ethanol.

4. Conclusions

In this work, experimental LTHR results of binary mixtures of iso-octane, and ethanol were obtained using a motored engine with inlet temperatures of 40 °C to 140 °C at equivalence ratios of 0.5, 0.67 and 1.0 with boosted (1.5 barA) conditions.. Both pressure-derived and carbon monoxide emission measurements were used to determine LTHR intensity. These experimental results were analysed with the help of ignition delay contours, and a sensitivity analysis, obtained from accompanying chemical kinetics modelling.

The results show that:

- Exhaust carbon monoxide concentration is proportional to the heat released from LTHR for each fuel and equivalence ratio group.
- Blending ethanol into iso-octane in relatively small quantities has drastic inhibiting effects on the blend's LTHR behaviour—much more than can be accounted for by the displacement of iso-octane molecules by non-LTHR exhibiting molecules. Blends of 20% vol ethanol exhibited no LTHR at the conditions tested.
- The Livengood-Wu integral has been shown to be a good predictor of LTHR occurrence, given the pressure-temperature history of a mixture.
- The differences in first stage ignition delay times of the fuels—and ultimately the behaviour observed in this work can be explained by the effect of ethanol's introduction on the pool of OH radicals, which are heavily involved in the initiation of low temperature oxidation of iso-octane (by hydrogen abstraction) and the subsequent chain branching reactions related to LTHR.

5. Nomenclature

ACI	Advanced compression ignition
AHRR	Apparent heat release rate
AI	Autoignition
°CA	Crank angle degrees
CA50	CA location at 50% heat release point
CAI	Controlled autoignition
CHR	Cumulative heat release
CO	Carbon monoxide
EVC	Exhaust valve closing
EVO	Exhaust valve opening
GCI	Gasoline compression ignition
HCCI	Homogenous charge compression ignition
ICE	Internal Combustion Engine
IVC	Intake valve closing
IVO	Intake valve opening
k	Chemical reaction rate
LTHR	Low temperature heat release
LW	Livengood-Wu progress variable
NTC	Negative temperature coefficient
OExx	Iso-octane ethanol blend with xx %vol ethanol
P	Pressure
PRF	Primary reference fuel
SI	Spark ignition
T	Temperature
TDC	Top dead centre
V	Volume
ϕ	Fuel-air equivalence ratio

τ Ignition delay time

6. Acknowledgements

This research was supported by an Engineering and Physical Sciences Research Council Prosperity Partnership, grant number EP/T005327/1. For the purpose of Open Access, the authors have applied a CC BY public copyright license to any Author Accepted Manuscript (AAM) version arising from this submission. The Prosperity Partnership is a collaboration between JLR, Siemens Digital Industries Software, the University of Bath, and the University of Oxford. The authors would also like to thank the Dept. of Engineering Science technicians and maintenance teams for facilities support.

References

[1] F. Leach, G. Kalghatgi, R. Stone, P. Miles, The scope for improving the efficiency and environmental impact of internal combustion engines, Transportation Engineering 1 (2020) 100005. doi:https://doi.org/10.1016/j.treng.2020.100005.
URL https://www.sciencedirect.com/science/article/pii/S2666691X20300063

[2] P. Iodice, M. Cardone, Ethanol/gasoline blends as alternative fuel in last generation spark-ignition engines: A review on co and hc engine out emissions, Energies 14 (13) (2021).
URL https://www.mdpi.com/1996-1073/14/13/4034

[3] S. Kim, B. Dale, Ethanol fuels: E10 or e85 – life cycle perspectives (5 pp), The International Journal of Life Cycle Assessment 11 (2) (2006) 117–121. doi:10.1065/lca2005.02.201.
URL https://doi.org/10.1065/lca2005.02.201

[4] K. Senecal, F. Leach, Racing Toward Zero: The Untold Story of Driving Green, SAE International, 2021.

[5] W. P. Attard, H. Blaxill, A lean burn gasoline fueled pre-chamber jet ignition combustion system achieving high efficiency and low nox at part load, in: SAE 2012 World Congress and Exhibition, SAE International, 2012. doi:10.4271/2012-01-1146.
URL 10.4271/2012-01-1146

[6] A. U. Bajwa, F. C. P. Leach, M. H. Davy, Prospects of controlled auto-ignition based thermal propulsion units for modern gasoline vehicles, Energies 16 (9) (2023). doi:10.3390/en16093887.
URL https://www.mdpi.com/1996-1073/16/9/3887

[7] W. R. Leppard, The chemical origin of fuel octane sensitivity, in: International Fuels and Lubricants Meeting and Exposition, SAE International, 1990. doi:https://doi.org/10.4271/902137.

[8] Astm d2699-19e1, standard test method for research octane number of spark-ignition engine fuel, Standard,

ASTM International, West Conshohocken, PA (2019).

[9] Astm d2700-19e1, standard test method for motor octane number of spark-ignition engine fuel, Standard, ASTM International, West Conshohocken, PA (2019).

[10] F. Battin-Leclerc, Detailed chemical kinetic models for the low-temperature combustion of hydrocarbons with application to gasoline and diesel fuel surrogates, Progress in Energy and Combustion Science 34 (4) (2008) 440–498. doi:https://doi.org/10.1016/j.pecs.2007.10.002.
URL https://www.sciencedirect.com/science/article/pii/S0360128507000627

[11] G. E. Bogin, J. Luecke, M. A. Ratcliff, E. Osecky, B. T. Zigler, Effects of iso-octane/ethanol blend ratios on the observance of negative temperature coefficient behavior within the ignition quality tester, Fuel 186 (2016) 82–90. doi:https://doi.org/10.1016/j.fuel.2016.08.021.
URL https://www.sciencedirect.com/science/article/pii/S0016236116307578

[12] E. Singh, M. Waqas, B. Johansson, M. Sarathy, Simulating hcci blending octane number of primary reference fuel with ethanol, in: WCX 17: SAE World Congress Experience, SAE International, 2017. doi:https://doi.org/10.4271/2017-01-0734.
URL https://doi.org/10.4271/2017-01-0734

[13] E. Singh, E.-A. Tingas, D. Goussis, H. G. Im, S. M. Sarathy, Chemical ignition characteristics of ethanol blending with primary reference fuels, Energy & Fuels 33 (10) (2019) 10185–10196. doi:10.1021/acs.energyfuels.9b01423.

[14] G. Shibata, K. Oyama, T. Urushihara, T. Nakano, Correlation of low temperature heat release with fuel composition and hcci engine combustion,, SAE Technical Paper (2005). doi:https://doi.org/10.4271/2005-01-0138.

[15] M. Mehl, W. Pitz, M. Sjöberg, J. Dec, Detailed kinetic modeling of low-temperature heat release for prf fuels in an hcci engine, 2009. doi:10.4271/2009-01-1806.

[16] G. Shibata, K. Oyama, T. Urushihara, T. Nakano, The effect of fuel properties on low and high temperature heat release and resulting performance of an hcci engine, in: SAE 2004 World Congress Exhibition, SAE International, 2004. doi:https://doi.org/10.4271/2004-01-0553.

[17] I. Truedsson, W. Cannella, B. Johansson, M. Tuner, Engine speed effect on auto-ignition temperature and low temperature reactions in hcci combustion for primary reference fuels, in: SAE 2014 International Powertrain, Fuels Lubricants Meeting, SAE International, 2014. doi:https://doi.org/10.4271/2014-01-2666.

[18] Y. Yang, J. E. Dec, N. Dronniou, M. Sjöberg, Tailoring hcci heat-release rates with partial fuel stratification: Comparison of two-stage and single-stage-ignition fuels, Proceedings of the Combustion Institute 33 (2) (2011) 3047–3055. doi:https://doi.org/10.1016/j.proci.2010.06.114.
URL https://www.sciencedirect.com/science/article/pii/S1540748910001999

[19] M. R. Saxena, S. Rana, R. K. Maurya, Analysis of Low- and High-Temperature Heat Release in Dual-Fuel RCCI

Engine and Its Relationship With Particle Emissions, Journal of Energy Resources Technology 144 (9) (2022) 091201. arXiv:https://asmedigitalcollection.asme.org/energyresources/article-pdf/144/9/091201/6855894/jert_144_9_091201.pdf, doi:10.1115/1.4053517.

[20] R. Willems, F. Willems, N. Deen, B. Somers, Heat release rate shaping for optimal gross indicated efficiency in a heavy-duty rcci engine fueled with e85 and diesel, Fuel 288 (2021) 119656. doi:https://doi.org/10.1016/j.fuel.2020.119656.

[21] S. L. Kokjohn, R. M. Hanson, D. A. Splitter, R. D. Reitz, Fuel reactivity controlled compression ignition (rcci): a pathway to controlled high-efficiency clean combustion, International Journal of Engine Research 12 (3) (2011) 209–226. arXiv:https://doi.org/10.1177/1468087411401548, doi:10.1177/1468087411401548.

[22] D. A. Splitter, A. Gilliam, J. Szybist, J. Ghandhi, Effects of pre-spark heat release on engine knock limit, Proceedings of the Combustion Institute 37 (4) (2019) 4893–4900. doi:https://doi.org/10.1016/j.proci.2018.05.145.

[23] D. Splitter, B. Kaul, J. Szybist, G. Jatana, Engine operating conditions and fuel properties on pre-spark heat release and spi promotion in si engines, SAE International Journal of Engines 10 (3) (2017) 1036–1050.
URL https://www.jstor.org/stable/26285109

[24] M. Yamakawa, T. Youso, T. Fujikawa, T. Nishimoto, Yoshitaka, gt;Wada, K. Sato, H. Yokohata, Combustion technology development for a high compression ratio si engine, SAE International Journal of Fuels and Lubricants 5 (1) (2012) 98–105.
URL http://www.jstor.org/stable/26272866

[25] S. White, A. Bajwa, F. Leach, Isolated low temperature heat release in spark ignition engines, in: WCX SAE World Congress Experience, SAE International, 2023.

[26] A. Bajwa, S. White, F. Leach, Low temperature heat release and phi-sensitivity characteristics of iso-octane/air mixtures, Combustion Science and Technology (2023).

[27] J. P. Szybist, D. A. Splitter, Pressure and temperature effects on fuels with varying octane sensitivity at high load in si engines, Combustion and Flame 177 (2017) 49–66. doi:https://doi.org/10.1016/j.combustflame.2016.12.002.

[28] F. Leach, M. Davy, M. Peckham, Cyclic no2:nox ratio from a diesel engine undergoing transient load steps, International Journal of Engine Research 22 (1) (2021) 284–294. arXiv:https://doi.org/10.1177/1468087419833202, doi:10.1177/1468087419833202.
URL https://doi.org/10.1177/1468087419833202

[29] N. Papaioannou, F. C. Leach, M. H. Davy, A. Weall, B. Cooper, Evaluation of exhaust gas recirculation techniques on a high-speed direct injection diesel engine using first law analysis, Proceedings of the Institution of Mechanical Engineers, Part D: Journal of Automobile Engineering 233 (3) (2019) 710–726. arXiv:https://doi.org/10.1177/0954407017749110, doi:10.1177/0954407017749110.

URL https://doi.org/10.1177/0954407017749110

[30] D. Bresenham, J. Reisel, K. Neusen, Spindt air-fuel ratio method generalization for oxygenated fuels, SAE Transactions 107 (1998) 2154–2171.
URL http://www.jstor.org/stable/44736682

[31] C. R. Stone, Introduction to Internal Combustion Engines, 4th Edition, Macmillan International Higher Education, 2012.

[32] Y. Wu, P. Pal, S. Som, T. Lu, A skeletal chemical kinetic mechanism for gasoline and gasoline/ethanol blend surrogates for engine cfd applications, 2017.

[33] U. Burke, W. K. Metcalfe, S. M. Burke, K. A. Heufer, P. Dagaut, H. J. Curran, A detailed chemical kinetic modeling, ignition delay time and jet-stirred reactor study of methanol oxidation, Combustion and Flame 165 (2016) 125–136. doi:https://doi.org/10.1016/j.combustflame.2015.11.004.
URL https://www.sciencedirect.com/science/article/pii/S0010218015003958

[34] B. Weber, High pressure ignition chemistry of alternative fuels, Ph.D. thesis, University of Connecticut (06 2014).

[35] L. Chen, R. Stone, Measurement of enthalpies of vaporization of isooctane and ethanol blends and their effects on pm emissions from a gdi engine, Energy & Fuels 25 (3) (2011) 1254–1259. doi:10.1021/ef1015796.

[36] H. Curran, P. Gaffuri, W. Pitz, C. Westbrook, A comprehensive modeling study of iso-octane oxidation, Combustion and Flame 129 (3) (2002) 253–280. doi:https://doi.org/10.1016/S0010-2180(01)00373-X.
URL https://www.sciencedirect.com/science/article/pii/S001021800100373X